

Accurate Modeling of Unusual Electronic Circuit Elements with Artificial Neural Networks

Ladislav Pospíšil, Josef Dobeš, and Abhimanyu Yadav

Czech Technical University in Prague, Faculty of Electrical Engineering, Department of Radio Engineering

Technická 2, 166 27 Praha 6, Czech Republic

Email: {pospis1,dobes,yadavabh}@fel.cvut.cz

Abstract—Nowadays, there are many various electronic structures for which their nonlinear models for CAD are necessary, especially for microwave ones. However, in the recent PSpice-family programs, only a class of five types of the MESFET model is available. In the paper, a new method is suggested for modeling miscellaneous electronic structures by exclusive neural networks, or by corrective neural networks working attached to a conveniently modified analytic model. The accuracy of the proposed modification of the analytic model is assessed by extracting the model parameters of GaAs MESFET, AlGaAs/InGaAs/GaAs pHEMT, and GaAs microwave varactors. The accuracy of the procedures that use the neural networks is assessed by extracting element's model parameters in static and dynamic domains. First, a precise approximation of the pHEMT output characteristics is carried out by means of both exclusive and corrective artificial neural networks; and second, an approximation of the capacitance (C-V) function of the SACM InGaAs/InP avalanche photodiode is performed by the exclusive neural network. Last, the Pt–TiO_{2-x}–Pt memristor characteristic with an extraordinary (but typical) hysteresis is approximated by a set of cooperative artificial neural networks, as a single network is unable to characterize this unconventional element.

Keywords—Artificial neural networks, MESFET, pHEMT, microwave varactor, memristor, optimization, parameter extraction.

I. INTRODUCTION

FOR CHARACTERIZING the electronic devices, there exist a number of models of various complexities [1]–[12], where the last two ones also contain valuable comparisons of them. In [11], both DC and capacitance parts of four models are compared using a set of measurements, and in [12], properties of DC characteristics of nine models are compared using a submicron GaAs MESFET. The realistic model of Parker and Skellern [7] can be considered most precise one, however, the identification of its model parameters is often too complicated and therefore not realized [13]. For this reason, the authors frequently seek to improve a classic model adding some function(s) with fitting parameter(s) [8]–[10], [12].

A. Analytic Models and Using Artificial Neural Networks

Modeling of microwave devices by artificial neural networks in general is described in [14]. Various types of modeling the semiconductor devices by artificial neural networks are also described in [15]–[20] – [15] presents a neural network approach for TCAD empirical modeling, [16] presents a modeling procedure for the HEMT transistors, [17] presents MOSFET and BJT AC/DC modeling, [18] presents the small and large signal models for an AlGaAs and a SiGe HBT, [19] presents Schottky diode and pHEMT linear/nonlinear modeling, and [20] presents a new approach to implement neural networks models for MOSFET into SPICE.

B. Suggested Methods of Improving the Model Accuracy

First, an improvement of a classic model is suggested. The Sussman-Fort, Hantgan, and Huang [1] model equations have been selected as a good compromise between complexity and accuracy. Therefore, they can be used as an appropriate base for a corrective neural network, but both DC and capacitance part of them must be conveniently modified in advance for modeling the special microwave elements as pHEMT or varactor. The suggested improvement consists in addition of two new model parameters: the first enables characterization of possible negative output conductance, and the second enables modeling highly nonlinear capacitances of the widely various class of microwave varactors.

However, the accuracy of the modified functions is still of a percentage order in both DC and capacitance part of the model. To be more precise, using both exclusive neural network and corrective neural network with this modified analytic model can be considered an efficient and relatively simple way.

II. MODIFYING THE ANALYTIC MODEL OF MESFET

The diagram of the MESFET model in Fig. 1 is applicable for characterizing majority of microwave transistors.

A. Modifying the DC Part of the MESFET Model

The *primary* voltage-controlled current source of the MESFET model I_d can be defined for the forward mode ($V_d \geq 0$) by standard formulae [1], [6] with a simple but efficient modification:

$$V_T = V_{T0} - \sigma V_d, \quad (1a)$$

$$I_d = \begin{cases} 0 & \text{for } V_g \leq V_T, \\ \beta (V_g - V_T)^{n_2} (1 + \lambda V_d) \tanh(\alpha V_d) & \text{otherwise,} \end{cases} \quad (1b)$$

and by mirrored equations for the reverse mode ($V_d < 0$)

$$V_T = V_{T0} + \sigma V_d, \quad (2a)$$

$$I_d = \begin{cases} 0 & \text{for } V'_g \leq V_T, \\ \beta (V'_g - V_T)^{n_2} (1 - \lambda V_d) \tanh(\alpha V_d) & \text{otherwise,} \end{cases} \quad (2b)$$

where $V'_g = V_g - V_d$. The model parameters V_{T0} , β , n_2 , λ , and α are generally known [1], [6], the parameter σ used in (1a) and (2a) represents the simple but important modification necessary for modeling potential negative conductance in the MESFET output characteristics.

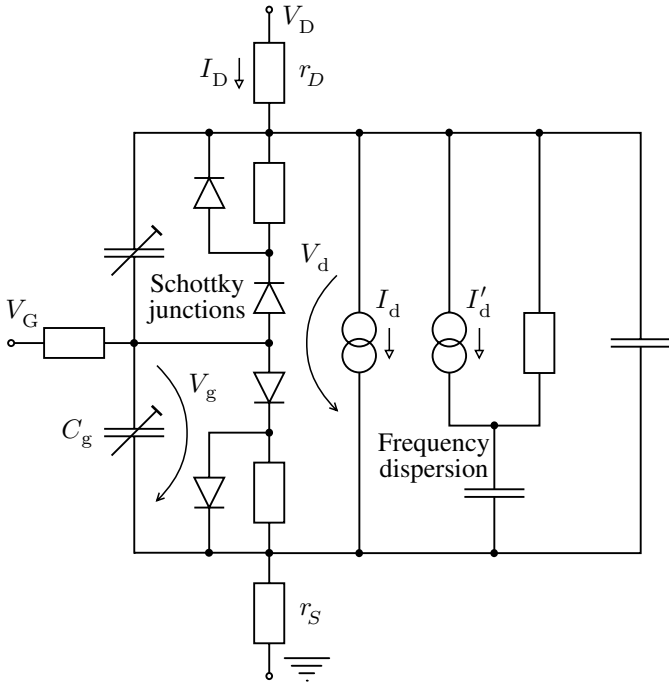


Fig. 1. Diagram of the MESFET model with the frequency dispersion.

Although the equations (1) and (2) are relatively very simple, they contain an important improvement in comparison with the classic Curtice model [4] (by n_2 parameter which characterizes gate-voltage influence on I_d more precisely), and also in comparison with the classic Statz model [2] (by σ parameter which characterizes drain-voltage influence on I_d more precisely).

A comparison of our model based on the slightly modified equations (1) and (2) with eight other ones is performed in [12] in a comprehensive way.

The importance of the modifications (1a) and (2a) can be clearly demonstrated by the identification of the model parameters for DZ71 MESFET [3], which is shown in Fig. 2. The C.I.A. optimization procedure [10] has determined the values of the model parameters $V_{T0} = -1.36$ V, $\beta = 0.0346$ A V $^{-2}$, $n_2 = 1.73$, $\lambda = -0.082$ V $^{-1}$ (note that the negative value of this parameter sometimes arises if the parameter σ is used), $\alpha = 2.56$ V $^{-1}$, $\sigma = 0.141$, $r_D = 2.88$ Ω , and $r_S = 2.62$ Ω (note that the r_D and r_S parameters have already been estimated in [3]). To compare the achievement, the parameters of the same MESFET have also been identified for the classical Statz model [2]. As shown in Fig. 2, the modified formulae are more accurate, especially for the lesser values of the gate-source control voltage, and also for the greater values of the drain current.

B. Using the Modified Model as a PHEMT Approximation

The modifications (1a) and (2a) enable the model to be used as the pHEMT approximation, which is shown in Fig. 3. The parameter extraction process has determined the values $V_{T0} = -1.64$ V, $\beta = 0.102$ A V $^{-2}$, $n_2 = 0.991$, $\lambda = -0.0288$ V $^{-1}$, $\alpha = 1.16$ V $^{-1}$, $\sigma = 0.00797$, $r_D = 0.3$ Ω , and $r_S = 0.2$ Ω .

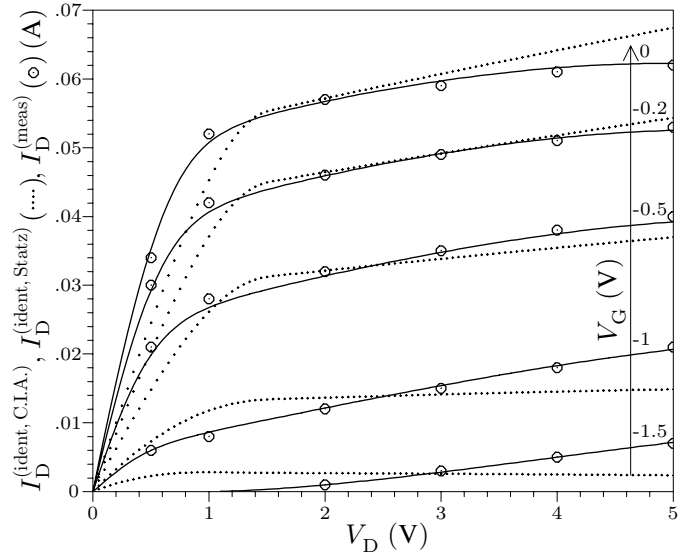


Fig. 2. Comparison of the MESFET model identification using formula (1) (continuous lines) and the classical Statz equation (dots) [2]. The root-mean-square and maximal-absolute-value deviations (see the definitions in Appendix) of the model (1) are $rms = 2.73$ % and $\delta_{max} = 8$ %, respectively. The measured data (circled dots) is taken from [3].

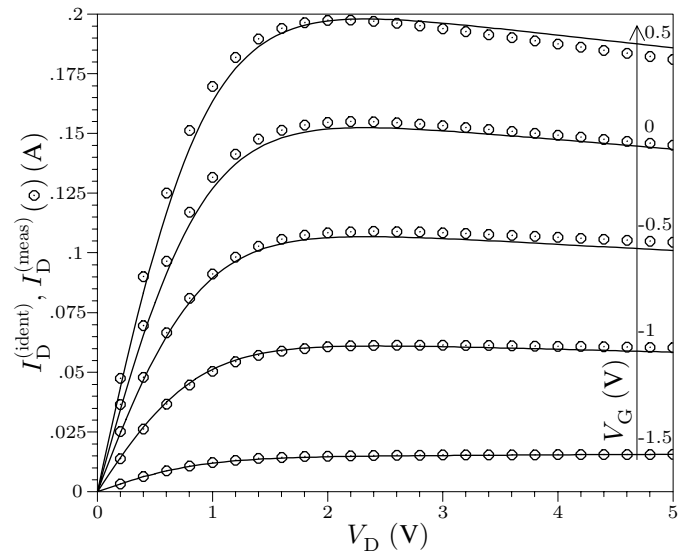


Fig. 3. Results of the AlGaAs/InGaAs/GaAs power pHEMT model identification (continuous lines) using formula (1) ($rms = 2.38$ % and $\delta_{max} = 8.24$ %). The measured data (circled dots) is taken from [8].

This model represents the transistor with the rms deviation of a percentage order, and is slightly more accurate than the TriQuint one [8].

On the other hand, at very high frequencies, the values of the s_{22} parameter does *not* match the DC curves. Therefore, a *secondary* current source I'_d must be added, and its model parameters can be identified using a system of the s parameters of pHEMT at various operating points.

C. Modifying the Capacitance Part of the MESFET Model

In general, the MESFET gate capacitances are highly non-linear as shown in Fig. 4. The model of the gate-source

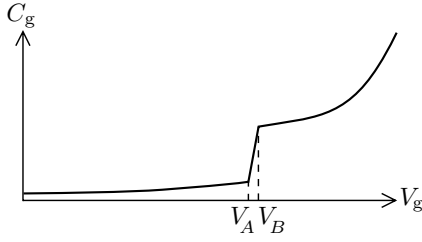


Fig. 4. Nonlinear MESFET capacitance model (for both source and drain junctions).

capacitance splits into the three parts, similar to those in the Statz [2] and recent models [7]:

$$C_g = \begin{cases} \epsilon W \arctan \sqrt{\frac{\phi_0 - V_T}{V_T - V_g}} & \text{for } V_g \leq V_A, \\ \frac{V_g - V_A}{V_B - V_A} \left[C_{J0} \left(1 - \frac{V_B}{\phi_0} \right)^{-m} + \right. \\ \left. \pi \frac{\epsilon W}{2} - \epsilon W \arctan \sqrt{\frac{\phi_0 - V_T}{V_T - V_A}} \right] + \\ \epsilon W \arctan \sqrt{\frac{\phi_0 - V_T}{V_T - V_A}} & \text{for } V_g > V_A \wedge \\ & V_g < V_B, \\ \pi \frac{\epsilon W}{2} + C_{J0} \left(1 - \frac{V_g}{\phi_0} \right)^{-m} & \text{for } V_g \geq V_B, \end{cases} \quad (3)$$

where the transitional region (V_A, V_B) is specified empirically:

$$V_A = V_T - 0.15 \text{ V}, \quad V_B = V_T + 0.08 \text{ V}. \quad (4)$$

All the model parameters have already been defined in [1] with the exception of the power $-m$ (the classic models including the Statz one always use the theoretical value $-\frac{1}{2}$ instead of $-m$).

D. Using the Modified Model as a Varactor Approximation

The microwave varactors are highly nonlinear with observed voltage dependencies analogical to those in the MESFET gate capacitances. Therefore, the functions in (3) can be used after replacing C_g and V_g with the external ones, i.e., with C_G and V_G . Let us emphasize that such empirical method is often used in the microwave semiconductor device modeling.

First, let us demonstrate this idea by identifying the Texas Instruments EG8132 [21] gate varactor model as shown in Fig. 5. The identification results confirm that the use of (3) enables more accurate approximation than the 6th-order polynomial in [21]. The optimization procedure of the C.I.A. program has determined the values of the model parameters $\epsilon W = 0.15711$ pF, $C_{J0} = 1.0771$ pF, $V_T = -2.7569$ V, $\phi_0 = 23.451$ V, and $m = 12.827$. Emphasize that the last two parameters do not have “physical” values, which clearly illustrates the necessity of using the $-m$ -power in (3).

Second, for the EG8132 source varactor, the optimization procedure of the C.I.A. program has determined the values of the model parameters $\epsilon W = 0.13587$ pF, $C_{J0} = 0.66625$ pF, $V_T = -2.6026$ V, $\phi_0 = 13.251$ V, and $m = 8.1457$ with a

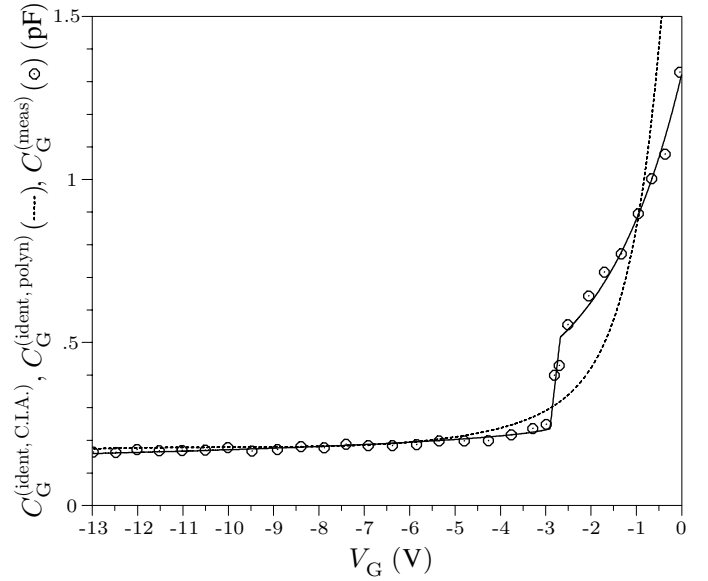


Fig. 5. Comparison of the Texas Instruments EG8132 *gate*-varactor model identification using formula (3) and a polynomial approximation (rms = 4.52 % and $\delta_{\max} = 13.7$ % for (3)). The measured data (circled dots) is taken from [21], where the polynomial approximation $a_0 + a_2(V_G - V_A)^{-2} + a_3(V_G - V_A)^{-3} + \dots + a_6(V_G - V_A)^{-6}$ has been demonstrated with the results drawn by the dashed line. (In [21], the parameters $V_A = -8$ V, $a_0 = -0.54$ pF, $a_2 = 2.3$ nF V², $a_3 = -87.938$ nF V³, $a_4 = 1.4$ μ F V⁴, $a_5 = -10.458$ μ F V⁵, and $a_6 = 30.48$ μ F V⁶ have been used for the interpolation polynomial.)

little more precise device characterization as shown in Fig. 6 – let us compare the values rms and δ_{\max} .

Third, the parameters of the capacitance model of the optical SACM (Separated Absorption, Charge, and Multiplication) avalanche photodiode MO457/4 (International Laser Centre [22]) have also been extracted. The optimization procedure of the C.I.A. program has determined the values of the model parameters $\epsilon W = 1.51155$ pF, $C_{J0} = 5.30894$ pF, $V_T = -6.17455$ V, $\phi_0 = 204.491$ V, and $m = 30.4842$ with a little lesser accuracy as shown in Fig. 7. Therefore, potential improvement of this (not excellent) model using an artificial neural network is advisable, and it will be demonstrated in Section III.

III. APPLYING THE ARTIFICIAL NEURAL NETWORKS

The rms and δ_{\max} deviations from measured data for the analytic models can be of the percentage order, which was clearly illustrated in Section II. To obtain lesser values, the artificial neural networks can be used for modeling the devices. A detailed description of the concept of the neural networks can be found in [14] with the emphasis to modeling the nonlinear microwave devices. There can be two fundamental ways for using the artificial neural networks. The first consists in applying an exclusive neural network, i.e., it works *without* any analytic model, and the second uses a neural network as a correction tool for the *difference* between the measured data and the previously identified analytic model (which was suitably modified in advance).

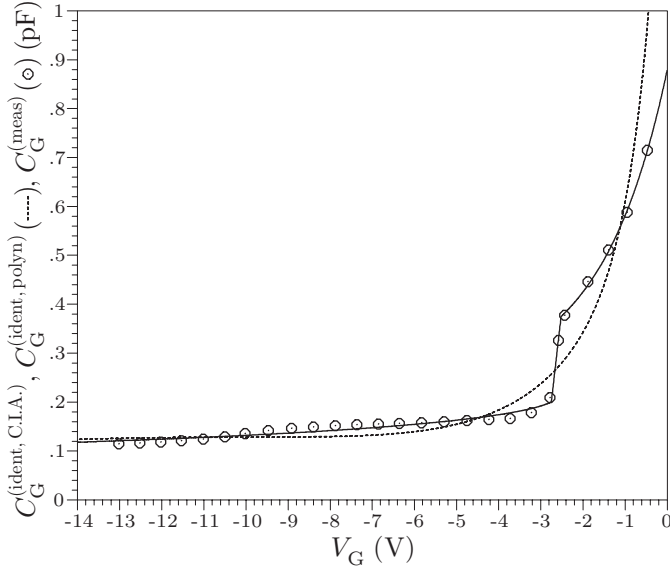


Fig. 6. Comparison of the EG8132 *source*-varactor model identification using formula (3) and the polynomial approximation (rms = 4 % and $\delta_{\max} = 6.87$ % for (3)). The measured data and the same polynomial approximation ($V_a = -6$ V, $a_0 = -0.09$ pF, $a_2 = 0.4783$ nF V², $a_3 = -14.703$ nF V³, $a_4 = 0.18351$ μ F V⁴, $a_5 = -1.0475$ μ F V⁵, and $a_6 = 2.3177$ μ F V⁶) are taken from [21] again.

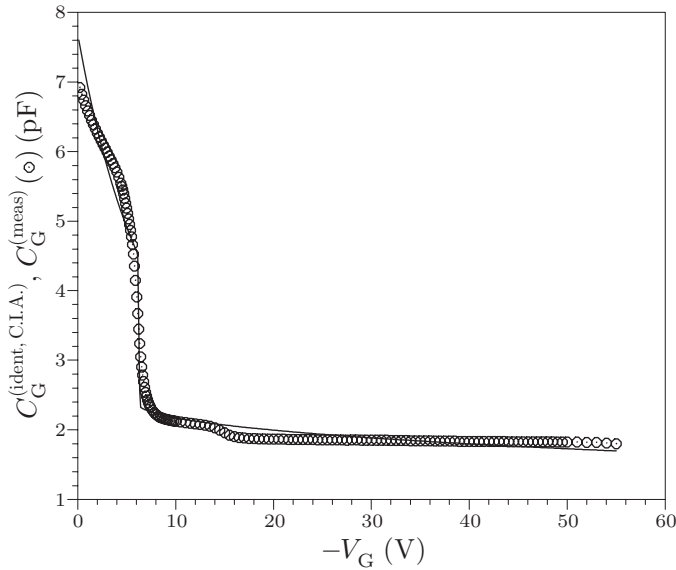


Fig. 7. Results of the MO457/4 capacitance model identification using formula (3) (rms = 6.21 % and $\delta_{\max} = 23.7$ %). The measured data has been granted by the authors of [22].

A. Applying the Exclusive Artificial Neural Networks

Initially, the models identified in Section II have also been approximated using the exclusive neural networks to compare their accuracy with the modified analytic models. Regarding the exclusive artificial neural networks, the standard multilayer perceptrons (MLP) structure [14, p. 65] has been used. The number of layers and the number of neurons in these layers have been selected performing greater number of systematic numerical tests.

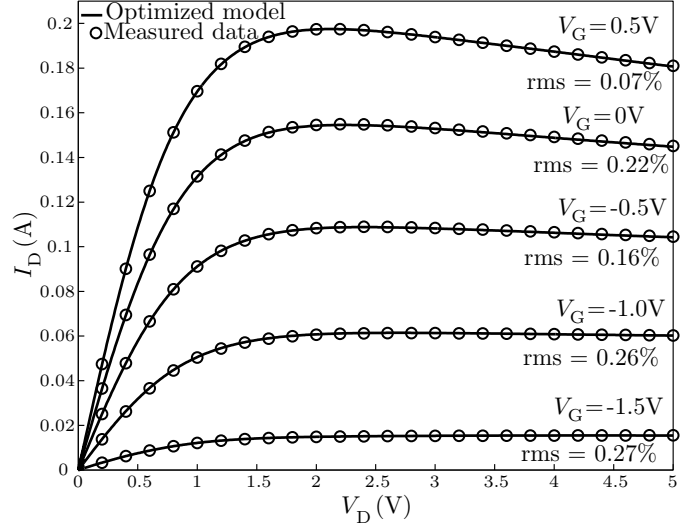


Fig. 8. Results of the pHEMT model identification using exclusive neural network of the MLP-2-5-4-5-1 structure (for all the characteristics together, rms = 0.2 %).

TABLE I
COMPARISON OF THE ACCURACY OF THE MODIFIED ANALYTIC MODEL WITH THE MODELS CREATED BY THE EXCLUSIVE AND CORRECTIVE NEURAL NETWORKS

V_G (V)	Analytic model	rms (%)	
		Exclusive	Corrective
0.5	3.23	0.07	0.0006162
0	2.68	0.22	0.0005629
-0.5	2.39	0.16	0.0014
-1	1.85	0.26	0.0362
-1.5	1.23	0.27	0.1043
All curves	2.38	0.2	0.028

1) *Enhancing the Accuracy of the PHEMT Model:* The exclusive artificial neural network has also been used for modeling the pHEMT with the results shown in Fig. 8 and the third column of Table I. A relatively simple structure MLP-2-5-4-5-1 has been selected. As shown in Table I, the accuracy of the exclusive neural network (rms = 0.2 %) has been approximately ten times better than that for the modified analytic model (rms = 2.38 %).

2) *Enhancing the Accuracy of the Varactor Model:* The optical SACM avalanche photodiode MO457/4 [22] model should be replaced by a neural network because the approximation by the analytic function (3) was not ideal (the values of rms and δ_{\max} mentioned in Fig. 7). For characterizing this photodiode, a simple structure MLP-1-4-5-4-1 has been used with the result shown in Fig. 9. Let us emphasize that the accuracy of this exclusive neural network is sufficient – hence, there is no need to use a corrective neural network in a combination with the analytic model here.

B. Applying the Corrective Artificial Neural Network

In Fig. 10, only the *differences* between the pHEMT measured data and previously identified analytic model are shown (circles) and approximated using a corrective neural network (continuous lines). (In other words, in the first step an analytic

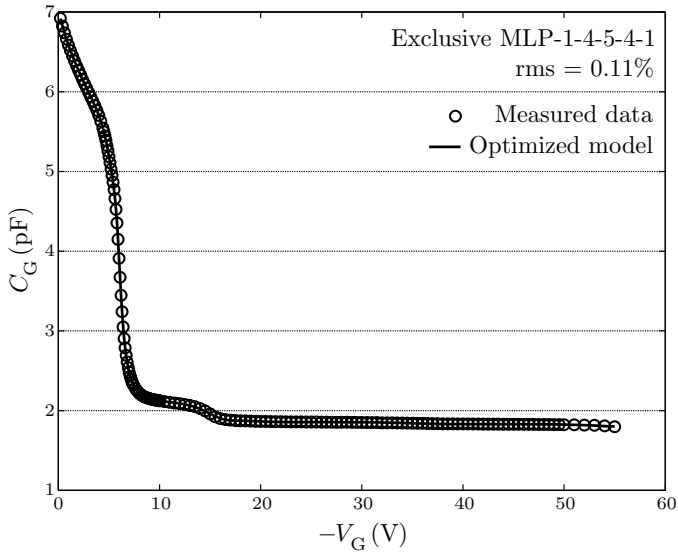


Fig. 9. Results of the MO457/4 capacitance model identification using exclusive neural network (δ_{\max} is only 0.4 %).

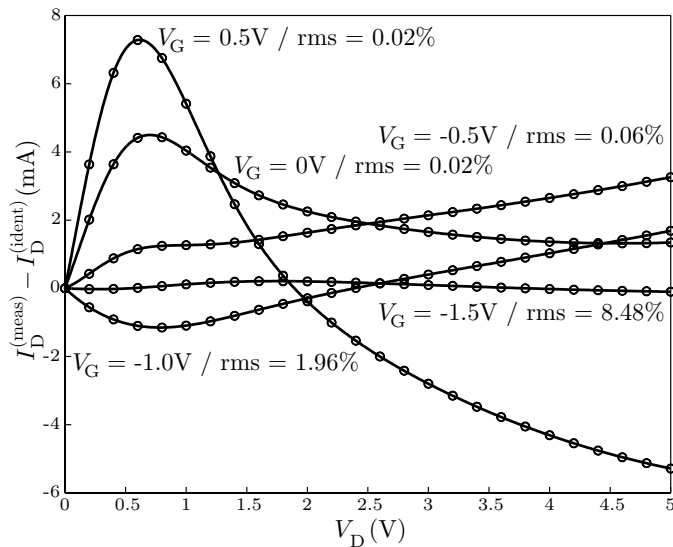


Fig. 10. Results of the approximation of the differences between the measured data and (previously identified) modified analytic model (that is shown in Fig. 3), which is an outcome of the corrective neural network MLP 2-8-10-6-1. (1000 training epochs have been used.)

model is identified, and its model parameters are extracted. After that, an error of the analytic model is evaluated. Finally, this error is compensated by a neural network.) The resulting accuracy of the modified analytic model with this corrective neural network is shown in the last column of Table I (the analytic model and corrective neural network operate together and therefore their final rms is much lesser than the rms of the differences). This methodology gives the best accuracy.

C. Applying the Cooperative Artificial Neural Networks

In Fig. 11, a set of measured points for a Pt – TiO_{2-x} – Pt memristor [23] is depicted. There are some analytic approximations of this characteristic with an extraordinary hysteresis and several irregularities [23], [24], but the precision of these

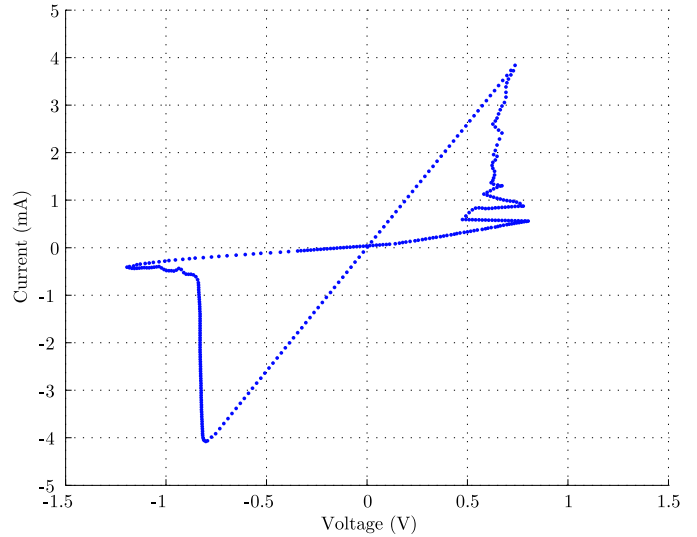


Fig. 11. Measured characteristic of a Pt – TiO_{2-x} – Pt memristor. Original characteristic and other technological data are described in all details in [23].

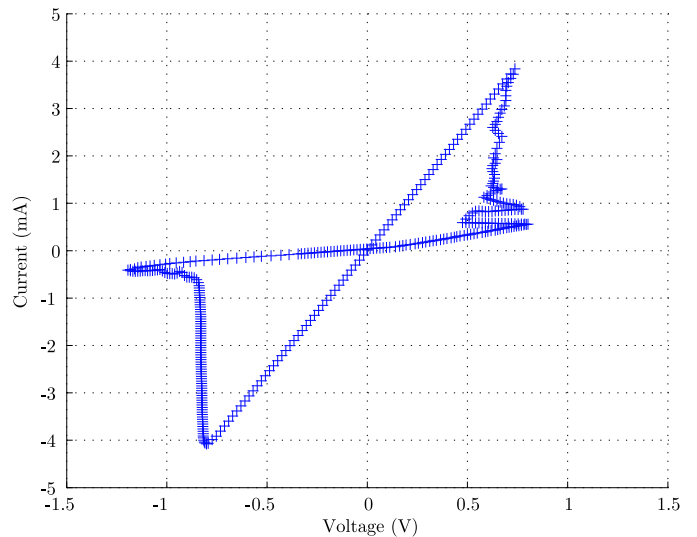


Fig. 12. An approximation of the memristor with a set of cooperative artificial neural networks, both $y = f(x)$ and $x = f(y)$ types of the networks are necessary because any single network is unable to characterize it precisely.

simple models is limited. Such an element is very difficult to be characterized especially with respect to the fact that it is neither $y = f(x)$ nor $x = f(y)$ function. For this reason, the element has been approximated by *more* cooperative networks, some of them of $y = f(x)$ and another one of $x = f(y)$ types.

The result of the usage of the set of the neural networks is shown in Fig. 12. For the comprehensive characterization of the memristor, the MLP-1-2-3-2-1 ($y = f(x)$, the low-resistance linear part), MLP-1-4-5-3-2-1 ($x = f(y)$, the most complicated part on the right), MLP-1-5-7-3-1 ($y = f(x)$, the analogical part on the left), and MLP-1-3-4-2-1 ($y = f(x)$, the high-resistance linear part) networks have been used, i.e., three or four (due to the most complicated part) internal layers have been necessary. As shown, the set of the cooperative networks is able to approximate the memristor in a quite precise way.

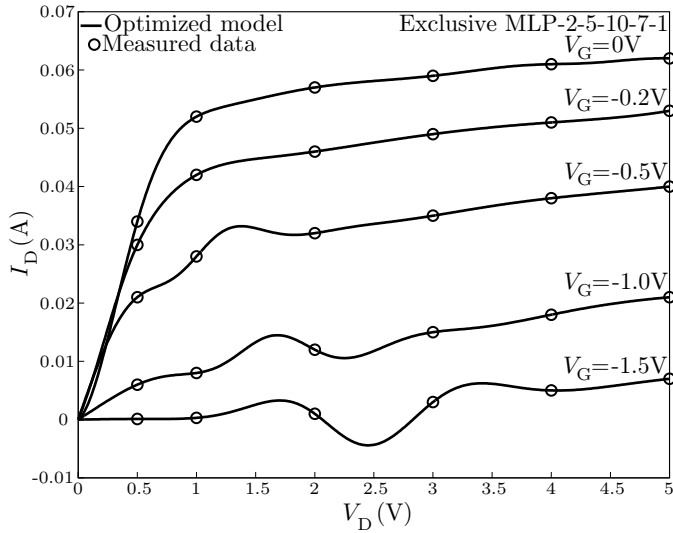


Fig. 13. Incorrect results of the DZ71 MESFET model identification caused due to an insufficient number of the measured points.

IV. CONCLUSIONS

The experiments confirm that the accuracy of the analytic models cannot be better than of a percentage order. Enhancing the precision is possible and relatively easy by artificial neural networks. Using the exclusive artificial neural networks gives the precision of tenths of percentage. However, the most accurate way consists in the combination of the modified analytic model with the corrective artificial neural network. Both analytic model parameters and neural network weights can easily be extracted using implemented optimization procedure.

For the elements with hysteresis and irregularities, an original method is suggested based on more cooperative networks.

ACKNOWLEDGMENT

This paper has been supported by the Grant Agency of the Czech Republic, grant No. P102/10/1614, and by the Czech Technical University Research Project No. MSM 6840770014 and the Ph.D. student grant No. SGS11/160/OHK3/3T/13.

APPENDIX

The **root-mean-square** and **maximal-absolute-value** deviations are defined by the formulae

$$\text{rms} = \sqrt{\frac{\sum_{i=1}^{n_p} \left(\frac{y_i^{(\text{ident})} - y_i^{(\text{meas})}}{y_i^{(\text{meas})}} \right)^2}{n_p}} \times 100 \%$$

and

$$\delta_{\max} = \max_{i=1, \dots, n_p} \left| \frac{y_i^{(\text{ident})} - y_i^{(\text{meas})}}{y_i^{(\text{meas})}} \right| \times 100 \%,$$

respectively, where $y_i^{(\text{ident})}$ and $y_i^{(\text{meas})}$ mark the identified and measured values, respectively, and n_p is the number of points.

The artificial neural networks must be used cautiously. The **devices must be measured in sufficient number of points.**

Otherwise, we could obtain bizarre results as shown for the DZ71 MESFET model identification in Fig. 13 – certainly, the number of measured points is absolutely insufficient for training the structure MLP-2-5-10-7-1.

REFERENCES

- [1] S. E. Sussman-Fort, J. C. Hantgan, and F. L. Huang, "A SPICE model for enhancement- and depletion-mode GaAs FET's," *IEEE Trans. Microwave Theory Tech.*, vol. 34, pp. 1115–1119, Nov. 1986.
- [2] H. Statz, P. Newman, I. W. Smith, R. A. Pucel, and H. A. Haus, "GaAs FET device and circuit simulation in SPICE," *IEEE Trans. Electron Devices*, vol. 34, pp. 160–169, Feb. 1987.
- [3] A. K. Jastrzebski, "Non-linear MESFET modeling," in *17th European Microwave Conference*, 1987, pp. 599–604.
- [4] W. R. Curtice, "GaAs MESFET modeling and nonlinear CAD," *IEEE Trans. Microwave Theory Tech.*, vol. 36, pp. 220–230, Feb. 1988.
- [5] A. Madjar, "A fully analytical AC large-signal model of the GaAs MESFET for nonlinear network analysis and design," *IEEE Trans. Microwave Theory Tech.*, vol. 36, pp. 61–67, Jan. 1988.
- [6] A. J. McCamant, G. D. McCormack, and D. H. Smith, "An improved GaAs MESFET model for SPICE," *IEEE Trans. Microwave Theory Tech.*, vol. 38, pp. 822–824, June 1990.
- [7] A. E. Parker and D. J. Skellern, "A realistic large-signal MESFET model for SPICE," *IEEE Trans. Microwave Theory Tech.*, vol. 45, pp. 1563–1571, Sept. 1997.
- [8] J. Cao, X. Wang, F. Lin, H. Nakamura, and R. Singh, "An empirical pHEMT model and its verification in PCS CDMA system," in *29th European Microwave Conference*, Munich, Oct. 1999, pp. 205–208.
- [9] D. H. Smith, "An improved model for GaAs MESFETs," TriQuint Semiconductors Corporation, Tech. Rep., 2000.
- [10] J. Dobeš, "C.I.A.—A comprehensive CAD tool for analog, RF, and microwave IC's," in *8th IEEE Int. Symp. High Performance Electron Devices for Microwave and Optoelectronic Applications*, Glasgow, Nov. 2000, pp. 212–217.
- [11] E. Sijercić and B. Pejcinović, "Comparison of non-linear MESFET models," in *9th IEEE Int. Conf. on Electronics, Circuits and Systems*, vol. III, Dubrovnik, Sep. 2002, pp. 1187–1190.
- [12] N. M. Memon, M. M. Ahmed, and F. Rehman, "A comprehensive four parameters $I-V$ model for GaAs MESFET output characteristics," *Solid-State Electronics*, vol. 51, no. 3, pp. 511–516, Mar. 2007.
- [13] B. Pejcinović, "Personal communication at ICECS," Sep. 2002.
- [14] Q. J. Zhang and K. C. Gupta, *Neural networks for RF and microwave design*. Boston: Artech House, 2000.
- [15] R. Matei, G. Dima, and M. D. Profirescu, "TCAD modeling using a neural network based approach," in *Modeling and Simulation of Microsystems*, 2001, pp. 518–521.
- [16] A. Caddemi and N. Donato, "Advanced simulation of semiconductor devices by artificial neural networks," *Journal of Computational Electronics*, vol. 2, pp. 301–307, 2003.
- [17] P. B. L. Meijer, "Neural network applications in device and subcircuit modelling for circuit simulation," Met lit. opg., Proefschrift Technische Universiteit Eindhoven, Philips Research Laboratories in Eindhoven, Netherlands, 2003.
- [18] K. Munshi, P. Vempada, S. Prasad, E. Sönmez, and H. Schumacher, "Small signal and large signal modeling of HBT's using neural networks," *Microwave Review*, vol. 9, no. 2, pp. 31–34, Dec. 2003.
- [19] X. Li, J. Gao, and G. Boeck, "Microwave nonlinear device modelling by using an artificial neural network," *Semicond. Sci. Technol.*, vol. 21, pp. 833–840, 2006.
- [20] H. B. Hammouda, M. Mhiri, Z. Gafsi, and K. Besbes, "Neural-based models of semiconductor devices for SPICE simulator," *American Journal of Applied Sciences*, vol. 5, no. 4, pp. 385–391, 2008.
- [21] C.-R. Chang, B. R. Steer, S. Martin, and E. Reese, "Computer-aided analysis of free-running microwave oscillators," *IEEE Trans. Microwave Theory Tech.*, vol. 39, pp. 1735–1744, Oct. 1991.
- [22] M. Klasovité, D. Haško, M. Tomáška, and F. Uherek, "Characterization of avalanche photodiode properties in frequency domain," in *5th Scientific Conference on Electrical Engineering & Information Technology*, Bratislava, Sep. 2002, pp. 63–65.
- [23] D. B. Strukov, G. S. Snider, D. R. Stewart, and R. S. Williams, "The missing memristor found," *Nature*, vol. 453, pp. 80–83, May 2008.
- [24] Z. Biolek, D. Biolek, and V. Biolková, "SPICE model of memristor with nonlinear dopant drift," *Radioengineering*, vol. 18, no. 2, part II, pp. 210–214, June 2009.